LU TP 15-nn
June 2015

Improving off-shell calculations of charged Higgs to quarks decays

Rasmus Hansen

Department of Astronomy and Theoretical Physics, Lund University

Bachelor thesis supervised by Johan Rathsman

Abstract

This paper presents some improvements to the method of calculating the partial width for decay of a charged Higgs particle, $H^{\pm}$, to a bottom quark and an off-shell top quark in a two Higgs doublet model (2HDM) as it is implemented in the program 2HDMC. The chief improvement is the addition of terms important for high values of $\tan\beta$ - the ratio between the two vacuum expectation values - and $m_{H^{\pm}} < m_t + m_b$. In addition, first-order QCD-corrections have been added to the method, and it has been extended to be applicable also below the threshold $m_{H^{\pm}} = m_t + m_b$. It also demonstrates how the inclusion of the top quark width-term in the propagator solves one of the problems with the old method of calculating the partial width in the program: a discontinuity in the partial width at $m_{H^{\pm}} = m_t + m_b$. Some other minor improvements have also been made: the method has been generalised to be valid for not only decay to t^*b, but also to t^*s and t^*d. The coupling constants have also been generalised to allow for 2HDM's that are not of the usual types I, II, X or Y. This enables non-zero off-diagonal elements in the inter-family coupling matrices that in turn allows for flavour-changing neutral currents at tree level, something that might be of interest in, for example, B to $D^{(*)}\tau\nu$-decays. These improvements will make it possible to set more reliable constraints and limits on the parameter space of the 2HDM. For example, it also affects the branching ratio of the charged Higgs decaying to a tau-lepton and a neutrino for $m_{H^{\pm}} < m_t + m_b$, although it is found that the effect is small. Even so the improvement opens up large regions in the parameter space to explore, some of them not available until now.

Contents

1 Introduction

When the Higgs particle was discovered in 2012[1][2] the weak gauge bosons (Z and $W^{\pm}$) and (most) fermions got their masses explained, but there are still issues left in the standard model (SM). Despite being an incredibly good description of most particle physics seen so far, there are still experimental results left unexplained by the SM, both 'minor' issues such as anomalous B-meson decays and more fundamental gaps such as gravity. This has encouraged physicists to seek other solutions. String Theory, Supersymmetry and quantum gravity are examples of theories that try to explain things the SM omits. String Theory was initially an attempt to explain hadrons, but quickly evolved into trying to unify all forces, Supersymmetry could potentially explain the so-called hierarchy problem and dark matter and quantum gravity is, just as the name suggests, the missing theory of quantum gravity. All of these, although still unproven, are candidates for being "the next big thing" in physics and should any of them be proven, it will surely be awarded a Nobel prize. To win a Nobel prize is hopefully not why most scientists do their research, but anything that warrants a Nobel prize is clearly a worthwhile endeavour.

The Two Higgs Doublet Model (2HDM) was initially introduced as an attempt to solve some of the issues of the SM, such as baryogenesis[5], as a new source of CP-violation. It does not open up many new fundamental doors that the SM Higgs mechanism does not already open, but from a phenomenological viewpoint it mostly supplies new decay paths for already existing particles. Although it may not be revolutionary, many other models, such as supersymmetry, require more Higgs particles than the SM can supply and a 2HDM is the easiest way to obtain these; in fact, the Minimal Supersymmetric Standard Model (MSSM) is a type of 2HDM.

The main feature of the 2HDM is that it contains five different Higgs particles: in the CP-conserving case there are two neutral CP-even scalar bosons, h and its heavier counterpart H, one neutral CP-odd scalar boson, A, and two charged scalar bosons, $H^{\pm}$. Normally, the neutral scalar h is identified as the one found in 2012. The other three are, as of mid-2015, still undiscovered. Experiments at CERN are searching for the new Higgs particles and data analyses have set constraints on their masses and the cross sections in various decay channels. When analysing data for the charged Higgs, the assumption that the decay channel $H^{\pm} \to \tau\nu$ dominates for $M_H^{\pm} < m_t + m_b$ is often made, but whether that is the case is one of the questions of which the improvements presented in this paper will enable investigation.

The purpose of this project has been to study the off-shell decays $H^{\pm} \to t^{*}b$ in 2HDMs in more detail and at the same time improve the method that calculates the partial decay width and branching ratio for $H^{\pm} \to t^{*}\overline{d}_i \to W^{\pm}b\overline{d}_i,\ d_i = (d, s, b)$ in the computer package 2HDMC[11]. In a kind of 2HDM called type II model, the decay width is roughly proportional to

$$\Gamma_{H^\pm}^{t^* d_i} \propto \cot^2 \beta m_t^2 + \tan^2 \beta m_{d_i}^2,$$

where $\tan \beta = \frac{v_2}{v_1}$ is the ratio between the two Higgs doublets vacuum expectation values (VEV), and the previous method in the program had omitted the latter part, $\tan \beta^2 m_{d_i}^2$, since the m_t^2-part is so much larger than the $m_{d_i}^2$-one for small values of $\tan \beta$. The asterisk on the top quark denotes that it is off-shell, i.e. $m_{H^\pm} < m_t + m_b$. Even though the decay channel is not allowed classically its phase space volume is still non-zero.

The paper is structured as follows: first the general procedure of how the Higgs mechanism and spontaneous symmetry breaking gives rise to massive vector bosons and the Higgs particle is covered in section 2. Section 3 is about the 2HDM, the interactions it allows, which symmetries one can apply and how that affects the parameters and the Yukawa couplings. How the width is calculated and which improvements has been done are discussed in section 4 and 5. Section 6 demonstrates the effect of the improvements and some example plots of the partial decays width and branching ratios for some values of $\tan \beta$ are presented in section 7. Section 8 presents a conclusion of the paper, and also covers an outlook on the future exploration of the 2HDM: further analysis of the parameter space of 2HDM and improving the calculations by improving the QCD-corrections.

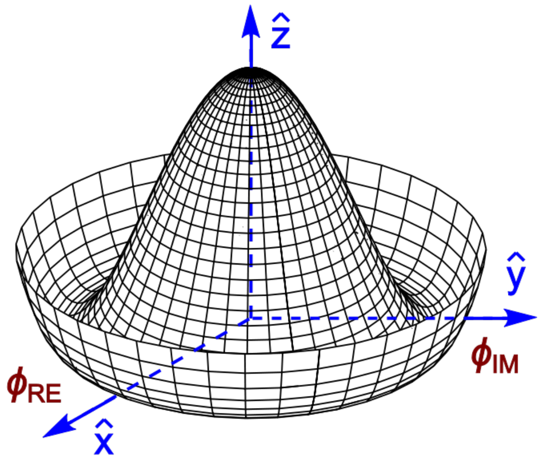

Figure 1: Graph of the Higgs potential for the complex scalar field that gets a VEV. Note that for two complex scalars the graph would in fact need to be four dimensional, something that is a bit tricky to represent graphically. The VEVs lies in the valley where the function takes its lowest values.[8]

2 The Higgs mechanism

As there are many good papers and books on the Higgs mechanism and spontaneous symmetry breaking (the books by Kane[4] and Griffiths[6], for example), this paper will not go into detail on this, instead it will just give a quick summary to remind the reader about the general procedure. For a more thorough guide The Higgs Hunters Guide[7] is a good option as it not only takes up the SM Higgs sector, but also extended Higgs sectors. One starts with a Lagrangian density that is given by

$$\mathcal{L} = \frac{1}{2}\partial_\mu \Phi^\dagger \partial^\mu \Phi + \frac{1}{2}\mu^2 \Phi^\dagger \Phi - \frac{1}{4}\lambda \left(\Phi^\dagger \Phi\right)^2, \tag{1}$$

where Φ is the Higgs field given by Eq.3 below, μ and λ are free parameters. The last two terms in the Lagrangian density correspond to the potential and it is minimized when

$$\Phi^\dagger \Phi = \frac{\mu^2}{\lambda} = v^2. \tag{2}$$

The minimum value v of the potential is called vacuum expectation value and it signals the spontaneous symmetry breaking. Since the Higgs potential takes the shape of a Mexican hat (it is sometimes called the Mexican hat-potential) there are a whole range of equally probable VEV's on a circle centered on the origin, as illustrated for an Abelian Higgs field in Fig.1. The general Higgs doublet is given by

$$\Phi = \begin{pmatrix} \phi_1 + i\phi_2 \\ \phi_3 + i\phi_4 \end{pmatrix}. \tag{3}$$

One can now choose a VEV and expand the Higgs potential around it, the most common choice is

$$\langle\Phi\rangle = \frac{1}{\sqrt{2}}\begin{pmatrix} 0 \\ v + h(x) \end{pmatrix}. \tag{4}$$

The symmetry from the ground state $\phi_i = 0$ is no longer present and the potential is no longer invariant under rotations.

For the Higgs field to be fully gauge invariant the derivative ∂_μ needs to be replaced by the covariant derivative $\mathcal{D}_\mu = \partial_\mu - ig_1\frac{Y}{2}B_\mu - ig_2\frac{\vec{\sigma}}{2}\cdot\vec{W}_\mu$, where g_1 and g_2 are coupling strengths of the U(1) and SU(2) groups, Y is the weak hypercharge, $\vec{\sigma}$ is a vector of the Pauli matrices and B_μ and $\vec{W}_\mu$ are the gauge fields from the U(1) and SU(2) groups, respectively. The physical fields Z_μ and A_μ, which correspond to the Z-boson and photon fields, are linear combinations of B_μ and W_μ^3 and defined as

$$\begin{aligned} A_\mu &= \frac{g_2 B_\mu - g_1 Y W_\mu^3}{\sqrt{g_2^2 + g_1^2 Y^2}}, \\ Z_\mu &= \frac{g_1 Y B_\mu - g_2 W_\mu^3}{\sqrt{g_2^2 + g_1^2 Y^2}} \end{aligned} \tag{5}$$

which leads to interaction terms between the Higgs and gauge bosons:

$$\left[\left(\partial_\mu - ig_1\frac{Y}{2}B_\mu - ig_2\frac{\vec{\sigma}}{2}\cdot\vec{W}_\mu\right)\Phi\right]^\dagger\left(\partial^\mu - ig_1\frac{Y}{2}B^\mu - ig_2\frac{\vec{\sigma}}{2}\cdot\vec{W}^\mu\right)\Phi. \tag{6}$$

For $\Phi = \frac{1}{\sqrt{2}}\binom{0}{v}$ this simplifies to the mass terms for Higgs and gauge bosons:

$$\begin{aligned} \left(\frac{1}{2}vg_2\right)^2 W_\mu^+ W^{-\mu} &\rightarrow m_W = \frac{1}{2}vg_2, \\ \frac{1}{2}\left(\frac{1}{2}v\sqrt{g_1^2+g_2^2}\right)^2 Z_\mu Z^\mu &\rightarrow m_Z = \frac{1}{2}v\sqrt{g_1^2+g_2^2}, \end{aligned} \tag{7}$$

and, as expected, no mass for the electromagnetic field.

2.1 Yukawa sector

The Yukawa sector of the Lagrangian completes this summary, and it is this part that gives rise to masses for all fermions, possibly except neutrinos. The Yukawa interaction for a single fermion generation is described by Stål in his doctoral thesis[9] and the Lagrangian is given by

$$\mathcal{L}_Y = -y_d\bar{q}_L\Phi d_R - y_u\bar{q}_L\tilde{\Phi}u_R - y_l\bar{l}_L\Phi e_R + h.c. \tag{8}$$

Here $\overline{q}_L = \binom{u_L}{d_L}$ and $u_{L,R}$ and $d_{L,R}$ are arbitrary up-type and down-type quarks of the same family, $\overline{l}_L = \binom{\nu_L}{e_L}$ and $e_{R,L}$ and ν_L are arbitrary leptons of the same family, the L and R subscripts denote the left- and right-handed parts of the fields and $\tilde{\Phi} = i\sigma_2\Phi^*$. It is not known whether ν_R actually exists since a right-handed neutrino has not yet been observed. By spontaneously breaking the electroweak symmetry, the mass terms for the fermions are found:

$$\frac{y_{u,d,l}v}{\sqrt{2}}(\overline{f}_L f_R + \overline{f}_R f_L) \to m_f = \frac{y_{u,d,l}v}{\sqrt{2}}. \tag{9}$$

We can now promote u_R, d_R and e_R to vectors in flavour space containing all three right-handed fermions of the families, $\overline{q}_L$ and $\overline{l}_L$ to vectors of the three left-handed doublets and $y_{u,d,l}$ to three 3×3 matrices in flavour space to obtain

$$\mathcal{L}_Y = -\overline{Q}_L Y_d \Phi D_R - \overline{Q}_L Y_u \tilde{\Phi} U_R - \overline{L}_L Y_l \Phi E_R + h.c., \tag{10}$$

where $U^T = (u, c, t)$, $\overline{Q}_L^T = ((u_L, d_L), (c_L, _L s), (t_L, b_L))$, similarly for D and L, and $Y_{u,d,l}$ are three 3×3 matrices. Note that U is different from lower case u used in Eq.8 as U is a vector containing all three up-type quarks while u is only a single quark, the same applies for down-type quarks and leptons as well. To find the mass eigenstates a bi-unitary transformation on the fermion fields needs to be done to diagonalise the mass-matrix:

$$M_f = \frac{v}{\sqrt{2}}(V_L^f)^\dagger Y_f V_R^f. \tag{11}$$

The down-type quarks and leptons are transformed in a similar fashion. As the up- and down-type quarks do not change exactly the same way under these transformations, i.e. their mass eigenstates are not related to their weak eigenstates in the same way, there is a small residue left that affects the flavour changing charged current. This residue is given by

$$V_{\text{CKM}} = (V_L^u)^\dagger V_R^d \tag{12}$$

and is called the Cabibbo-Kobayashi-Maskawa (CKM) matrix.

3 2HDM

By making the ansatz that, instead of just one, two complex scalar doublets are needed to fully describe the Higgs sector, one arrives at the result that five different Higgs particles must exist. For a more thorough plunge into the phenomenology, the review by Branco *et al*[15] and The Higgs Hunter's Guide[7] are good options while the papers by Oredsson[12] and Celis *et al*[13] give shorter reviews of the 2HDM. The most general form of these two doublets are

$$\Phi_1 = \begin{pmatrix} \phi_1 + i\phi_2 \\ \phi_3 + i\phi_4 \end{pmatrix} \rightarrow \langle \Phi_1 \rangle = \frac{1}{\sqrt{2}} \begin{pmatrix} 0 \\ v_1 \end{pmatrix} \qquad \Phi_2 = \begin{pmatrix} \phi_5 + i\phi_6 \\ \phi_7 + i\phi_8 \end{pmatrix} \rightarrow \langle \Phi_2 \rangle = \frac{1}{\sqrt{2}} \begin{pmatrix} 0 \\ v_2 \end{pmatrix}. \tag{13}$$

Just as for one Higgs doublet, Φ_1 and Φ_2 obtain VEV's, although they are not completely independent and are related to the VEV from the SM, v_{SM}, by

$$v_{SM} = v = \sqrt{v_1^2 + v_2^2}. \tag{14}$$

These two VEV's are in general complex numbers whose phases are unrelated to each other. By doing phase transformations to the fields Φ_1 and Φ_2 one can set one of the VEVs to be real, but both cannot be real at the same time unless they have the same phase. From here on $v_{1,2}$ are constrained to have the same phase and can thus be real at the same time. From Eq.14 the VEVs can be written as

$$\begin{aligned} v_1 &= v \cos\beta \\ v_2 &= v \sin\beta \\ \rightarrow \frac{v_2}{v_1} &= \tan\beta. \end{aligned} \tag{15}$$

By doing the same calculations with these doublets as one would do with a single Higgs doublet, i.e. minimising the potential, phase transforming to remove the imaginary part of the VEV and picking a 'direction' of the minimum, one will find that Φ_1 and Φ_2 can be expressed in terms of the physical Higgs fields as

$$\Phi_1 = \begin{pmatrix} -s_\beta H^+ \\ \frac{1}{\sqrt{2}}(c_\beta v - s_\alpha h + c_\alpha H - i s_\beta A) \end{pmatrix} \quad \Phi_2 = \begin{pmatrix} c_\beta H^+ \\ \frac{1}{\sqrt{2}}(s_\beta v - c_\alpha h + s_\alpha H + i c_\beta A) \end{pmatrix}. \tag{16}$$

Here four of the five Higgs particles can quickly be identified (h, H, A and H^+), the fifth is the complex conjugate of the charged and is, unsurprisingly, negatively charged. H and h are neutral CP-even scalar bosons, where h is usually identified to be the one found in 2012 at the LHC. A is a neutral CP-odd pseudo-scalar boson and $H^\pm$ are the two charged scalar bosons of which this paper is the focus. As with one Higgs doublet, the three remaining degrees of freedom gets 'eaten' by the $W^\pm-$ and Z-bosons, giving them mass. The angle α determines the mixing between the two neutral scalar Higgs particles, h and H and $\tan\beta = \frac{v_2}{v_1}$ is the ratio between the fields' VEVs. For simplicity, the notation $s_\alpha = \sin(\alpha)$, $c_\alpha = \cos(\alpha)$ etc. is used.

3.1 Free parameters and symmetries

The complete and most general renormalisable and gauge invariant potential of the Lagrangian density of the 2HDM is given by

$$
\begin{aligned}
V =& m_{11}^2\Phi_1^\dagger\Phi_1 + m_{22}^2\Phi_2^\dagger\Phi_2 - (m_{12}^2\Phi_1^\dagger\Phi_2 + h.c.) + \frac{1}{2}\lambda_1\left(\Phi_1^\dagger\Phi_1\right)^2 + \frac{1}{2}\lambda_2\left(\Phi_2^\dagger\Phi_2\right)^2 \\
&+ \frac{1}{2}\lambda_3\left(\Phi_1^\dagger\Phi_1\right)\left(\Phi_2^\dagger\Phi_2\right) + \frac{1}{2}\lambda_4\left(\Phi_1^\dagger\Phi_2\right)\left(\Phi_1^\dagger\Phi_2\right) \\
&+ \left\{\frac{1}{2}\lambda_5\left(\Phi_1^\dagger\Phi_2\right)^2 + \frac{1}{2}\lambda_6\left(\Phi_1^\dagger\Phi_1\right)\left(\Phi_1^\dagger\Phi_2\right) + \frac{1}{2}\lambda_7\left(\Phi_2^\dagger\Phi_2\right)\left(\Phi_1^\dagger\Phi_2\right) + h.c.\right\},
\end{aligned} \tag{17}
$$

and allows for a myriad of couplings. The parameters m_{11}, m_{22} and $\lambda_{1,2,3,4}$ are real and m_{12} and $\lambda_{5,6,7}$ are in the most general case complex. However, one can constrain the parameter space by requiring CP conservation and Z_2 symmetry, which removes 6 of the 14 (6 real and 4 complex parameters) degrees of freedom. CP conservation can be achieved by requiring all the parameters to be real[1]. Z_2 symmetry requires the potential to be invariant under

$$
\begin{aligned}
\Phi_1 &\to +\Phi_1 \\
\Phi_2 &\to -\Phi_2 \\
(U, D, E)_R &\to \pm(U, D, E)_R \\
(Q, L)_L &\to +(Q, L)_L,
\end{aligned} \tag{18}
$$

and for this to be fulfilled $\lambda_{6,7}$ and m_{12} needs to be zero. Although m_{12} breaks Z_2 symmetry, it only does it softly and the parameter can remain non-zero without breaking Z_2 symmetry. In practice, two additional degrees of freedom disappear due to that the SM Higgs mass and VEV are known from experiments.

3.2 Yukawa sector

Similarly to the SM case, the Yukawa sector of the 2HDM is given by

$$
\mathcal{L}_Y = -\overline{Q}_L(Y_1^d\Phi_1 + Y_2^d\Phi_2)D_R - \overline{Q}_L(Y_1^u\tilde{\Phi}_1 + Y_2^u\tilde{\Phi}_2)U_R - \overline{L}_L(Y_1^l\Phi_1 + Y_2^l\Phi_2)E_R + h.c. \tag{19}
$$

By using linear combinations of $Y_{1,2}^f$ given by

$$
\begin{aligned}
\kappa_0^f &= Y_1^f\cos\beta + Y_2^f\sin\beta \\
\rho_0^f &= -Y_1^f\sin\beta + Y_2^f\cos\beta,
\end{aligned} \tag{20}
$$

and replacing Φ_i with their respective VEV in Eq.19 all terms with ρ_0^f disappears and only κ_0^f remains. By doing a bi-unitary transformation on the fermion fields κ_0^f can be transformed into the mass matrix:

$$
M^f = \frac{v}{\sqrt{2}}\kappa^f = \frac{v}{\sqrt{2}}(V_L^f)\kappa_0^f V_R^f. \tag{21}
$$

[1]In principle a 2HDM can have CP conservation with complex parameters, but with real parameters there is certainly no CP violation.

In the general case, ρ_0^f is not diagonalisable at the same time as κ_0^f, but since ρ_f determines coupling within a family of fermions it might be desirable to have it diagonal, as that would eliminate any contribution to the flavour changing neutral current (FCNC) from the Higgs doublets. If they are simultaneously diagonalisable ρ^f and κ^f can be written as

$$\rho^f = \zeta_f \kappa^f. \tag{22}$$

By imposing a suitable Z_2 symmetry it is ensured that they are simultaneously diagonalisable, for example $U_R \to +U_R$ requires that $Y_2^u = 0$ since $\Phi_2 \to -\Phi_2$ as seen in Eq.18. Using Eq.20 with these requirements gives

$$\begin{cases} \kappa_0^u = Y_1^u \cos\beta \\ \rho_0^u = -Y_1^u \sin\beta \end{cases} \to \rho_0^u = -\tan\beta \kappa_0^u. \tag{23}$$

This procedure can be repeated with D and L to give relations between κ_0^d and ρ_0^d and κ_0^l and ρ_0^l. Technically this will give rise to 8 different types of 2HDM (3 choices of $\pm$), but since the choice to define v_1 and v_2 in Eq.15 is somewhat arbitrary there is in principle only 4. The values of the proportionality constants can be seen in Tab.1.

Model	ζ_d	ζ_u	ζ_l
Type I	cot(β)	cot(β)	cot(β)
Type II	-tan(β)	cot(β)	-tan(β)
Type X	cot(β)	cot(β)	-tan(β)
Type Y	-tan(β)	cot(β)	cot(β)

Table 1: Choices of $\zeta_{u,d,l}$ in different types of Z_2-symmetric 2HDMs. The type X model is sometimes called lepton specific and type Y flipped.

When Eq.22 is fulfilled the 2HDM is said to be Aligned. If ρ^f and κ^f does not fulfil Eq.22 ρ^f must have non-zero off-diagonal elements as when they are diagonalised the fields will get the mass eigenstates on the diagonal. Non-zero elements off the diagonal allow couplings of the type

$$\mathcal{L}_{\text{FCNC}} \propto u_i \Phi u_j.$$

i.e. FCNCs.

From this it is found that the couplings of the charged Higgs boson are given by[10]

$$\mathcal{L}_Y = -\overline{U}(V_{\text{CKM}}\rho^d P_R - \rho^u V_{\text{CKM}}^* P_L) D H^+ - \overline{\nu}\rho^L P_R L H^+ + h.c., \tag{24}$$

and the Feynman rules for quarks are

$$\begin{aligned} H^+\overline{u}_j d_i &: i\left[(\rho^u V_{\text{CKM}}^*)_{j,i} P_R - (V_{\text{CKM}}\rho^d)_{j,i} P_L\right], \\ H^- u_j \overline{d}_i &: i\left[(\rho^u V_{\text{CKM}}^*)_{j,i} P_L - (V_{\text{CKM}}\rho^d)_{j,i} P_R\right], \end{aligned} \tag{25}$$

where P_L and P_R are the left- and right-projection operators.

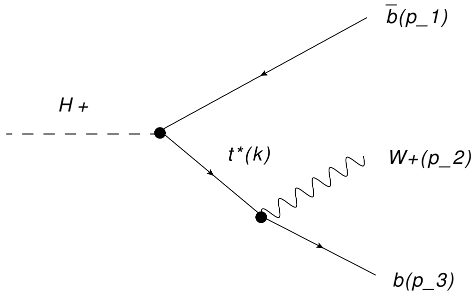

Figure 2: Feynman diagram for the decay $H^+ \to t^* \bar{b} \to W^+ \bar{b} b$.

4 How to calculate the partial width

To calculate the partial width and branching ratio of the decay $H^+ \to t^* b \to W^+ b b$, as illustrated in Fig.2, Eq. 20-24 from[13] was used:

$$\Gamma_{H^\pm}^{t^* b} = \frac{N_C G_F^2 |V_{tb}|^2}{16\pi^3 m_{H^\pm}^3} \int ds_{23} \int ds_{13} \frac{G(s_{23}, s_{13})}{(s_{23} - m_t^2)^2 \underline{+ \Gamma_t^2 m_t^2}}, \tag{26a}$$

where N_C is the number of colours, G_F is the Fermi constant, V_{tb} is the appropriate element in the CKM-matrix, $m_{H^\pm}$ is the mass of the charged Higgs particle, m_t is the mass of the top quark and Γ_t its decay width. In addition, s_{13} and s_{23} are the square of the total four-momentum for the $\bar{b}$ and b, and W^+ and b, respectively, as shown in Fig.2. The parts that are underlined have been changed from the original expression, as will be explained in section 5. The function G is given by

$$\begin{aligned} G(s_{23}, s_{13}) = &\left[m_W^2 (p_1 p_3) + 2(p_2 p_3)(p_1 p_2)\right] \cdot \left[\underline{|\zeta_u V_{tb}|^2 m_t^4} - \underline{|\zeta_d V_{tb}|^2 m_b^2} s_{23}\right] \\ &+ \left[m_W^2 (p_2 p_3 + m_b^2) + 2(p_2 p_3)(p_2 p_3 + m_W^2)\right] \cdot \\ &\cdot \left[2 \underline{m_b^2 |\zeta_d V_{tb}|^2} (p_1 p_2 + p_1 p_3) + 2 \underline{m_b^2 m_t^2 Re(\zeta_u \zeta_d^*) V_{tb}^2}\right], \end{aligned} \tag{26b}$$

The p_i are the momenta of the particles, $p_i p_j$ is the product of the four-momenta of particles i and j and the particles and momenta are related as: $\bar{b}(p_1)$, $W^\pm(p_2)$, $b(p_3)$ and $t^*(k) = t^*(p_2 + p_3)$. In the case $i = j$ the product becomes $p_i p_i = m_i^2$

$$\begin{aligned} (p_1 p_2) &= \frac{1}{2}(m_{H^\pm}^2 + m_b^2 - s_{13} - s_{23}), \\ (p_1 p_3) &= \frac{1}{2}(s_{13} - m_b^2 - \underline{m_{d_i}^2}) \\ (p_2 p_3) &= \frac{1}{2}(s_{23} - m_W^2 - m_b^2). \end{aligned} \tag{26c}$$

The integration limits are

$$(m_b + \underline{m_{d_i}})^2 \leq s_{13} \leq (m_{H^\pm} - m_W)^2$$

$$s_{23}^{min} = \left\{ \left(m_{H^\pm}^2 - m_W^2\right)^2 - \left[\lambda^{\frac{1}{2}}\left(m_{H^\pm}^2, s_{13}, m_W^2\right) + \lambda^{\frac{1}{2}}\left(s_{13}, m_b^2, \underline{m_{d_i}^2}\right)\right]^2 \right\} \tag{26d}$$

$$s_{23}^{max} = \left\{ \left(m_{H^\pm}^2 - m_W^2\right)^2 - \left[\lambda^{\frac{1}{2}}\left(m_{H^\pm}^2, s_{13}, m_W^2\right) - \lambda^{\frac{1}{2}}\left(s_{13}, m_b^2, \underline{m_{d_i}^2}\right)\right]^2 \right\},$$

where the Källén λ function is

$$\lambda(a, b, c) = a^2 + b^2 + c^2 - 2(ab + ac + bc). \tag{26e}$$

The integral is calculated numerically using the GSL library for C++, which uses the Gauss-Kronrod quadrature formula for approximating integrals and has been implemented in the program 2HDMC, replacing an old method that was only valid for Z_2-symmetric models and did not contain the terms proportional to ζ_d.

5 Changes to the calculation

When the method was implemented into 2HDMC it was evident that improvements were needed; the partial width $\Gamma_{H^\pm}^{t^*b}$ could not even be calculated for charged Higgs masses over $m_t + m_b$ as the integral in Eq.26b diverged.

One of the major contributions by this project is that the method is now accurate for large values of $\tan\beta$. This has been done by adding the terms containing ζ^d in Eq.26b and also generalising the $\zeta^{u,d}$-coefficients so that they need not be chosen from table 1. The original method used to calculate the width only included the first term in Eq.26b.

For the QCD-corrections each term in Eq.26b is multiplied by the relevant term out of

$$1 + \frac{4}{3}\alpha_S D_{\text{dup,udp,udm}}\left(s_{23}, m_{H^\pm}^2, m_b^2\right). \tag{27}$$

For more information on $D_{\text{dup,udp,udm}}$, see[16]. These QCD-corrections were initially calculated for on-shell top quarks, but by assuming that the off-shell top quark has a long enough lifetime the decay can still be regarded as a factorisation of two separate decays, one for $H^\pm \to t^*b$ and one for $t^* \to W^+b$. This approximation is not valid for $m_{H^\pm}$ much lower than $m_t + m_b$ as the top quarks' lifetime decreases the 'more off-shell' it is.

To avoid the pole at $\sqrt{s_{23}} = m_t$ the factor $\Gamma_t^2 m_t^2$ was added into the integral. This not only has the advantage of avoiding said pole, but it also makes the decay width continuous and usable over $m_{H^\pm} = m_t$, as Fig.3 and 4 will show later on, so that the function can be used both above and below the $m_{H^\pm} = m_t + m_b$-threshold. Even though the Γ_t should be calculated at every point in the integral for more accuracy, it was decided to focus on improving other parts of the method, so it is taken as constant and equal to the SM value. Even if Γ_t would have been calculated at every point it probably would have made little difference as it would just shift the peak of the $\frac{1}{(s_{23}-m_t^2)^2+\Gamma_t^2 m_t^2}$ slightly to higher $m_{H^\pm}$.

It is the up-type quark that determines whether or not the decay $H^\pm \to u_i d_j$ will contain an off-shell quark ($H^\pm \to (u,d)(d,s,b)$ will always be on-shell), as $m_{H^\pm}$ must be larger than 39.6GeV[14]. Thus the calculation in section 4 can be generalised to be valid also for $H^\pm \to t^* s$ and $H^\pm \to t^* d$ after some minor changes: m_b needs to be changed to m_{d_i} in the appropriate places and the V_{CKM}-element needs to be changed as it was described in section 3.2. Since these replacements already contain an element from the CKM-matrix squared, the power of $|V_{tb}|^2$ was reduced from 4 to 2 in Eq.26a.

From Eq.16 and 19 follows that every factor of $V_{tb}\zeta_u m_t$ and $V_{tb}\zeta_d m_{d_i}$ could be replaced by $(\rho^u V^*_{\text{CKM}})_{3,i}\frac{v}{\sqrt{2}}$ and $(V_{\text{CKM}}\rho^d)_{3,i}\frac{v}{\sqrt{2}}$ as $m_t = \kappa^u_{3,3}\frac{v}{\sqrt{2}}$, $m_{d_i} = \kappa^d_{i,i}\frac{v}{\sqrt{2}}$, $\zeta_u\kappa^u_{3,3} = (\rho^u V^*_{\text{CKM}})_{3,i}$ and $\zeta_d\kappa^d_{i,i} = (V_{\text{CKM}}\rho^d)_{3,i}$.

After the corrections were added, the function G (Eq.26b) looks like

$$\begin{aligned}
G(s_{23}, s_{13}) = &\left[m_W^2(p_1p_3) + 2(p_2p_3)(p_1p_2)\right]\cdot \\
&\cdot\left\{\left((\rho^u V^*_{\text{CKM}})_{3,i}\frac{v}{\sqrt{2}}\right)^2 m_t^2(1+\frac{4}{3}\alpha_S D_{udp}) - \right. \\
&\left. - \left((V_{\text{CKM}}\rho^d)_{3,i}\frac{v}{\sqrt{2}}\right)^2 s_{23}(1+\frac{4}{3}\alpha_S D_{dup})\right\} + \\
&+ \left[m_W^2(p_2p_3+m_b^2) + 2(p_2p_3)(p_2p_3+m_W^2)\right]\cdot \\
&\cdot\left\{2\left((V_{\text{CKM}}\rho^d)_{3,i}\frac{v}{\sqrt{2}}\right)^2(p_1p_2+p_1p_3)(1+\frac{4}{3}\alpha_S D_{dup}) + \right. \\
&\left. + 2m_{d_i}m_t\left((\rho^u V^*_{\text{CKM}})_{3,i}\frac{v}{\sqrt{2}}\right)\left((V_{\text{CKM}}\rho^d)_{3,i}\frac{v}{\sqrt{2}}\right)(1+\frac{4}{3}\alpha_S D_{udm})\right\}.
\end{aligned} \tag{28}$$

5.1 Implementation in the program

2HDMC is a program used to calculate partial decay widths for all five Higgs particles in a 2HDM, but it can also check the unitarity, perturbativity and stability of the model.

The original method in 2HDMC used three different calculations for different $m_{H^\pm}$:

1. $m_{H^\pm} < m_t + m_b$ without QCD-corrections.
2. $m_{H^\pm} > m_t + m_b$ with QCD-corrections.

3. $m_{H^\pm} \gg m_t + m_b$ in the massless limit with QCD-corrections.

The two latter partial widths were interpolated as

$$\Gamma_{H^\pm}^{t^*b} = \left(\frac{m_t + m_b}{m_{H^\pm}}\right)^2 \cdot \Gamma_2 + \left(1 - \left(\frac{m_t + m_b}{m_{H^\pm}}\right)^2\right) \cdot \Gamma_3. \tag{29}$$

where $\Gamma_{2,3}$ are the partial widths calculated using the second and third method above.

As the new method takes a long time to calculate the QCD-corrections it was decided to keep the fast method as an option in the program, although with some improvements in the $m_{H^\pm} < m_t + m_b$-range. In short, the two options are

- Faster, less precise and discontinuous method. This method is referred to as 'Fast method' in figures with graphs and has been improved somewhat in this paper.
    - New method when $m_{H^\pm} < m_t + m_b$ without QCD-corrections.
    - Method 2 and 3 from the original method when $m_{H^\pm} > m_t + m_b$ with QCD-corrections. In this interval these methods are interpolated with Eq.29.
- Slower, more precise and continuous method. This method is referred to as 'New method' in figures with graphs.
    - New method with QCD-corrections for all $m_{H^\pm}$. For $m_{H^\pm} > m_t + m_b$ it is interpolated with method 3 from the original method and interpolated with Eq.29.

6 The effect of the improvements

To illustrate the additions and how they improve the calculation the effect of each individual improvement is shown in Fig.3, where the partial width $\Gamma_{H^\pm}^{t^*b}$ has been calculated for $\tan\beta = 1, 50$ in the interval $150\text{Gev} < \mathrm{m_{H^\pm}} < 200\text{GeV}$. It is seen that, although not all improvements are significant for all masses and all values of $\tan\beta$, they are still necessary. The effects of QCD-corrections below $m_{H^\pm} = m_t + m_b$ can be seen in Fig.3 for $\tan\beta = 1$ as ζ_d has little impact for low values of $\tan\beta$, and Γ_t has little effect away from $m_{H^\pm} = m_t + m_b$. $\zeta_d \neq 0$ is primarily for large values of $\tan\beta$ and without it, the partial width is much smaller than it would have been otherwise for large $\tan\beta$, as Fig.3 shows that the partial width calculated with the new method is 3 orders of magnitude greater.

Fig.4 highlights the effect of adding the $m_t^2\Gamma_t^2$-term to the propagator. The fast method has a discontinuity at $m_{H^\pm} = m_t + m_b$ which is completely avoided by including the term in the propagator. The addition of this term was necessary as without it the partial width cannot be calculated at all, since Eq.26a diverges for $m_{H^\pm} > m_t$ without it, as shown in

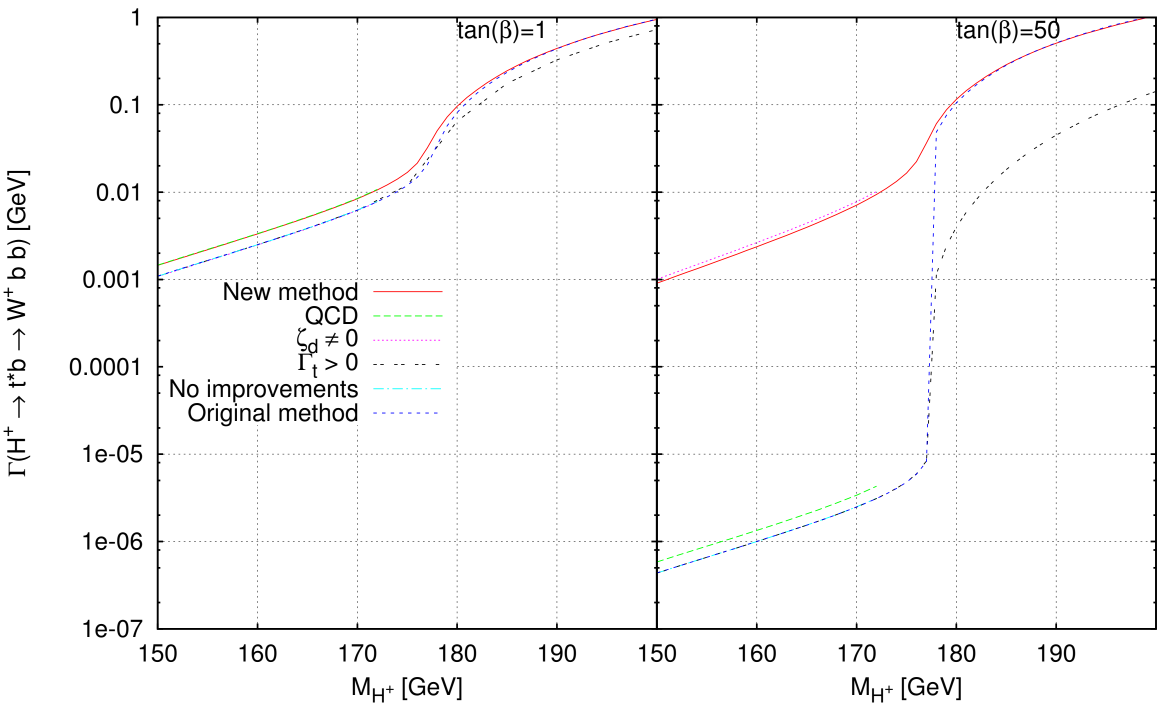

Figure 3: The effect of the improvements to the method of calculating $\Gamma^{t^*b}_{H^\pm}$. Graphs with $\Gamma_t = 0$ stretch to only $m_{H^\pm} = m_t$ as the integral diverges above that limit. The plots of each improvement is made with the other two off or disabled.

Fig.3. There is still a small notch, however, but this comes not from the propagator or any of the other improvements. It comes from that as soon as $m_{H^\pm} > m_t + m_b$ the new function is interpolated with the $m_{H^\pm} \gg m_t + m_b$-function. The black graph is the fast method and the red is the original method in the program before any improvements were made. These two methods use the same calculations when $m_{H^\pm} > m_t + m_b$ but different for $m_{H^\pm} < m_t + m_b$.

Unless otherwise stated, all calculations are done with $m_H = 400\ GeV$, $m_A = 500\ GeV$, $\sin(\beta - \alpha) = 0.999$, $\lambda_{6,7} = 0$ and $m_{12}^2 = 15800\ GeV^2$ in a type II model.

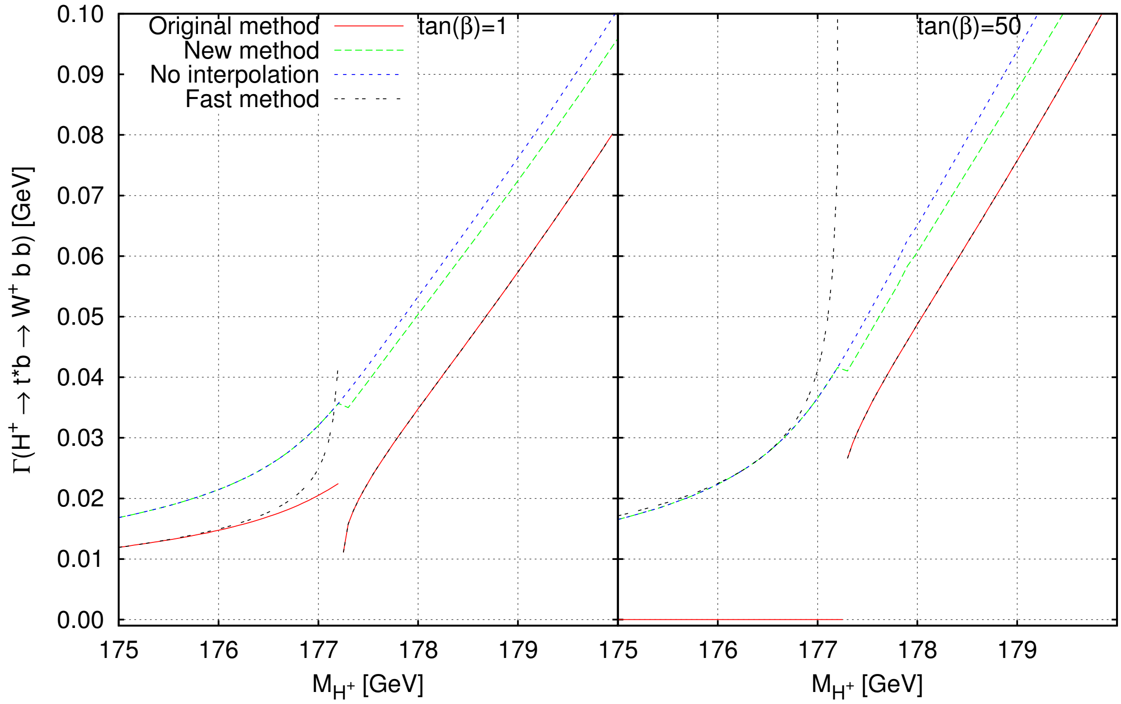

Figure 4: The partial width $\Gamma_{H^\pm}^{t^*b}$ zoomed in near the discontinuity of the original method in the program (red). For comparison, the new method with (green) and without (blue) the $m_{H^\pm} \gg m_t + m_b$-interpolation over the threshold and the fast method (black) are shown as well.

7 New values of branching ratios

7.1 Type II model

Fig.5 shows the branching ratio of $H^{\pm}$-decay to a bottom and an off-shell top quark for 100GeV $< m_{H^{\pm}} <$ 200GeV and Fig.6 shows the same decay channel for a higher range of $H^{\pm}$-masses: 100GeV $< m_{H^{\pm}} <$ 700GeV. In both figures the branching ratio has been calculated with both the new and the fast method. They clearly match very well and it would have taken a keen eye to differentiate between them had they not been coloured, other than right where $m_{H^{\pm}} = m_t + m_b$ and for low values of both $\tan\beta$ and $m_{H^{\pm}}$. The small difference in branching ratio in Fig.5 for $\tan\beta = 1$ is due to that, while both options use the same method, the faster option uses no QCD-corrections when $m_{H^{\pm}} < m_t + m_b$. As the mass increases $H^{\pm} \to W^{\pm}A$ and $H^{\pm} \to W^{\pm}H$ will take over and dominate instead of $H^{\pm} \to tb$. In Fig.5, for $\tan\beta = 7, 10$, one can faintly see a small dip in the green, fast method line. The dip comes from that the old $H^{\pm} \to t^{*}b \to W^{\pm}bb$-method is discontinuous at $m_{H^{\pm}} = m_t + m_b$, see Fig.4.

Note that, in Fig.5 and 6, only for $\tan\beta = 1$ is $BR(H^{\pm} \to t^{*}b \to W^{\pm}bb)$ large enough to give a significant contribution to the decay of the $H^{\pm}$, and unfortunately these values of $\tan\beta$ and $m_{H^{\pm}}$ are largely excluded in a type II model[3]. Despite that $BR(H^{\pm} \to t^{*}b \to W^{\pm}bb)$ is small for low $H^{\pm}$-masses, it is still non-zero and the new branching ratio for $H^{\pm} \to \tau^{\pm}\nu$ has been calculated and can be see in Fig.7.

As the branching ratio $H^{\pm} \to t^{*}b \to W^{\pm}bb$ is so small below the threshold it will have little impact on analyses of results from CERN for these choices of parameter values, but as this project has mainly been focused on improving the method for calculating the $H^{\pm} \to t^{*}b \to W^{\pm}bb$-width and not exploring the parameter space there are still many options left to cover.

In Fig.7, the branching ratio takes on the expected look, at least for $\tan\beta = 7, 10, 50$, of $1 - BR(H^{\pm} \to t^{*}b \to W^{\pm}bb)$ as often one assumes that $H^{\pm} \to \tau\nu$ is the only significant decay channel up until $m_{H^{\pm}} = m_t + m_b$, where $H^{\pm} \to t^{*}b \to W^{\pm}bb$ becomes important and dominates. The green line in Fig.7 shows $H^{\pm} \to \tau\nu$ for $\Gamma^{t^{*}b}_{H^{\pm}} = 0$ when $m_{H^{\pm}} < m_t + m_b$. If the width $H^{\pm} \to t^{*}b \to W^{\pm}bb$ is no longer zero for $m_{H^{\pm}} < m_t + m_b$, it should be the only other contributor than $H^{\pm} \to \tau\nu$. The small bump for $\tan\beta = 1$ at 172GeV comes from $H^{\pm} \to t^{*}(\overline{s}, \overline{d}) \to W^{\pm}b(\overline{s}, \overline{d})$, which will also become somewhat significant, although it is still suppressed due to the V_{CKM} matrix.

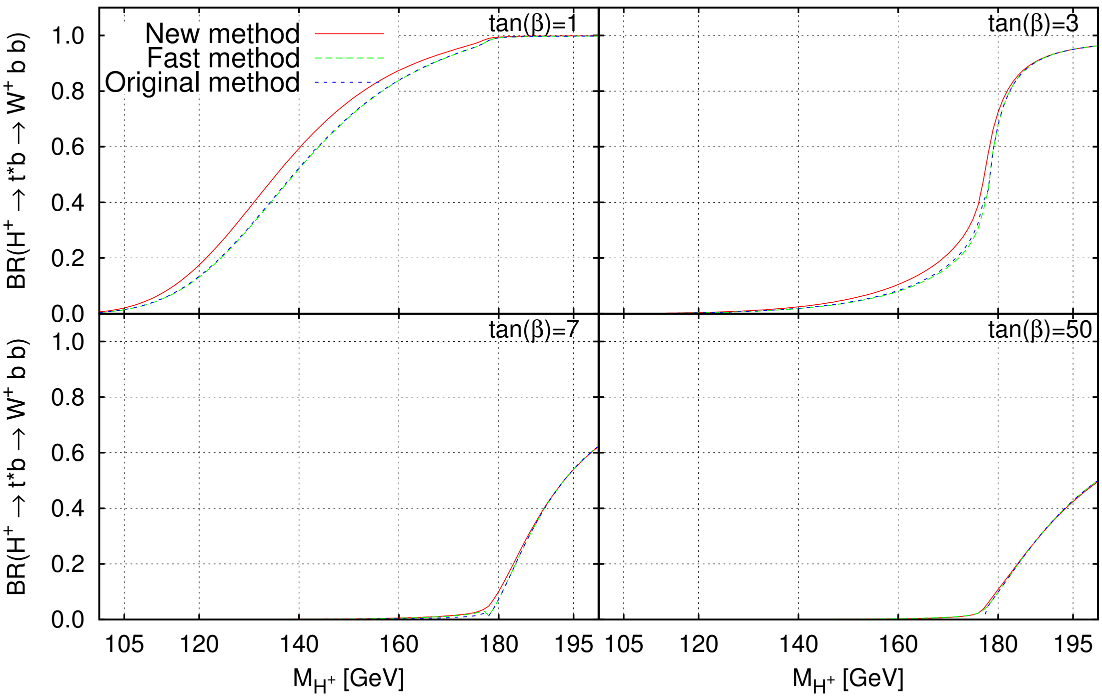

Figure 5: Calculated values of $BR(H^{\pm} \to t^{*}b \to W^{\pm}bb)$ for different values of $\tan\beta$. The data in these graphs are the same as in Fig.6, the only difference is the range in $m_{H^{\pm}}$-values.

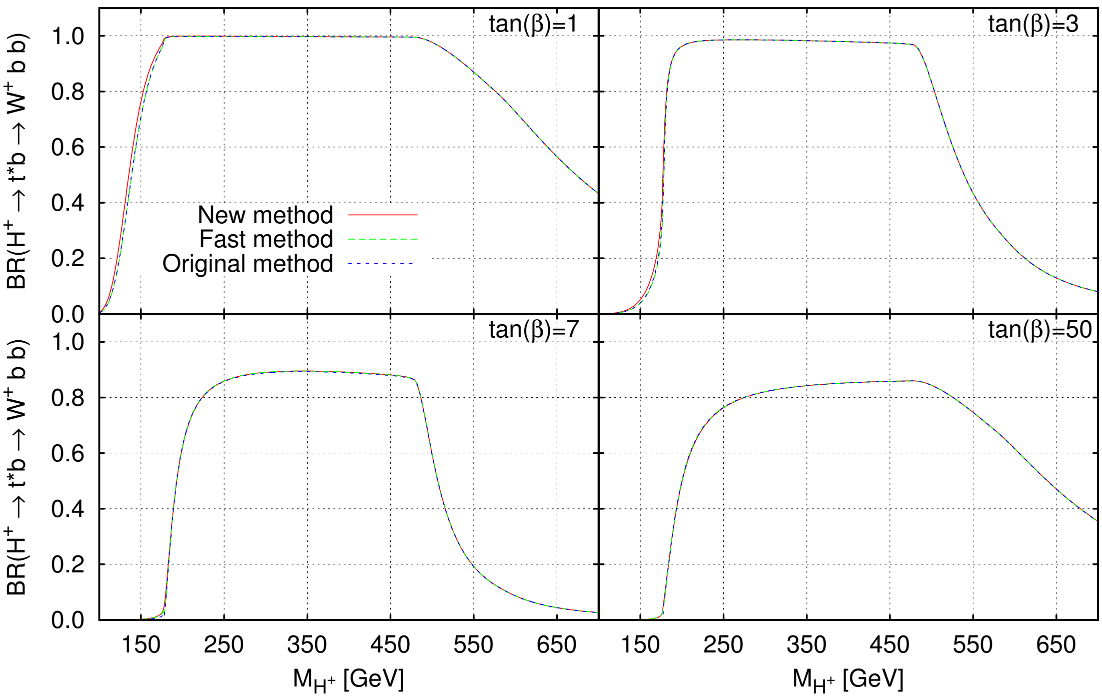

Figure 6: Calculated values of $BR(H^{\pm} \to t^{*}b \to W^{\pm}bb)$ for different values of $\tan\beta$.

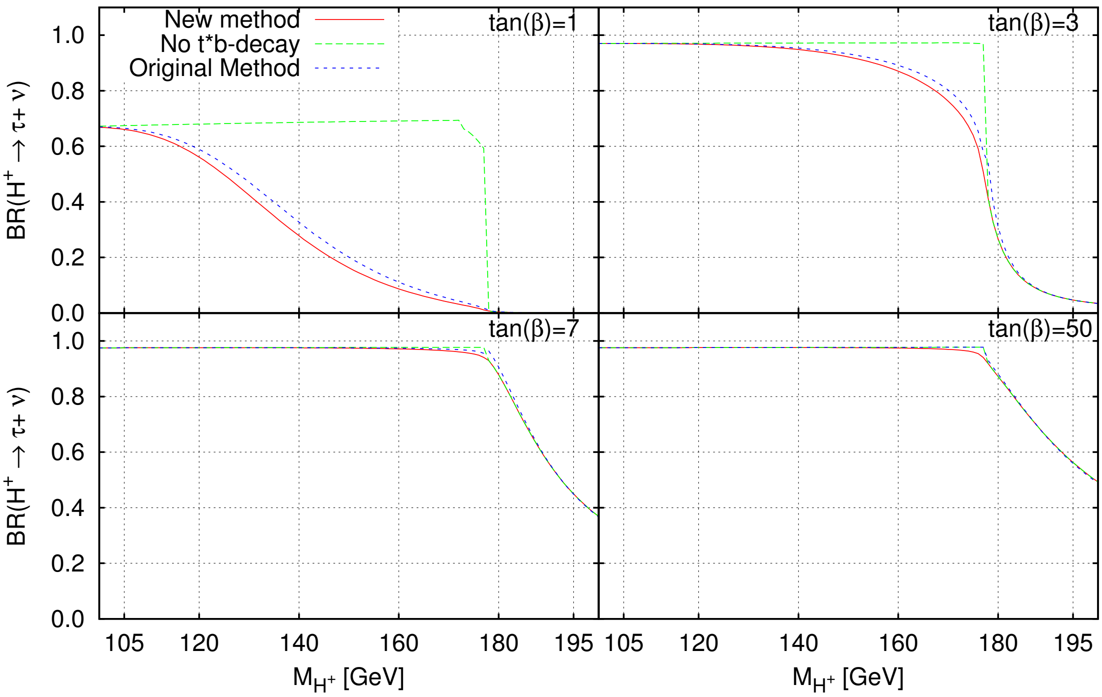

Figure 7: Calculated values of $BR(H^{\pm} \to \tau\nu)$. The green line is the branching ratio when $\Gamma^{t^*b}_{H^{\pm}} = 0$ for $m_{H^{\pm}} < m_t + m_b$ and $\Gamma^{t^*b}_{H^{\pm}} > 0$ above the threshold.

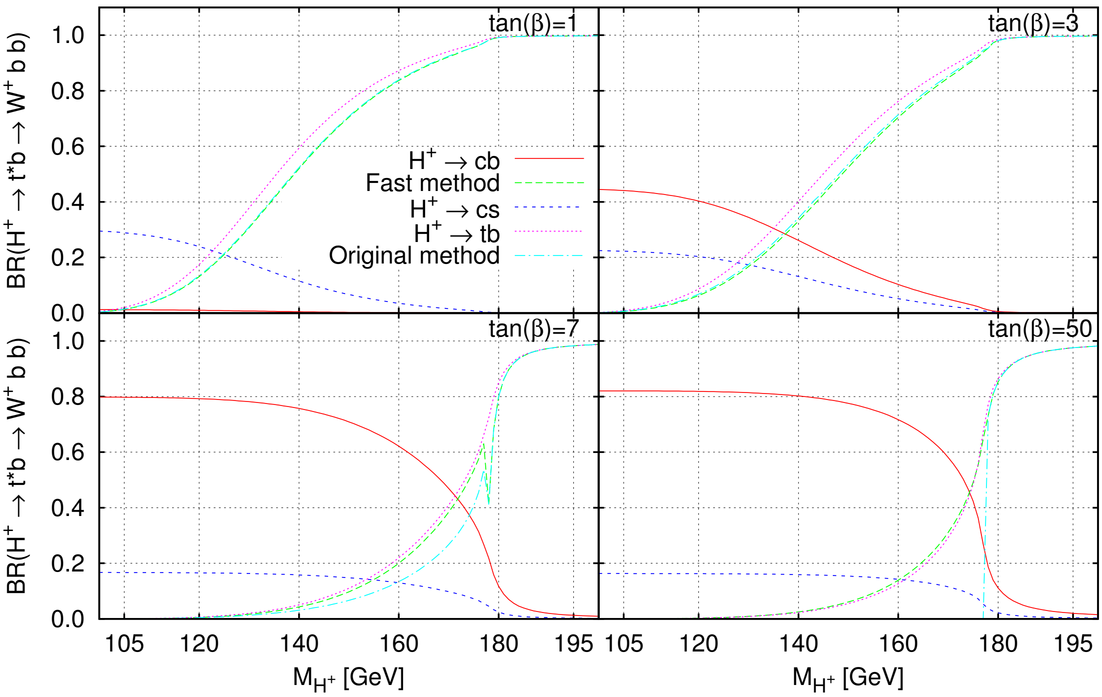

Figure 8: Calculated values of $BR(H^{\pm} \to t^{*}b \to W^{\pm}bb)$ for different values of $\tan\beta$ in a type Y/flipped 2HDM.

7.2 Type Y/flipped model

In the Type Y model the couplings to quarks are the same as in a Type II model while the couplings to the leptons has been flipped: $-\tan\beta \to \cot\beta$. In this type the quarks dominate the decay of $H^{\pm}$, as illustrated in 8.Although $H^{\pm} \to t^{*}b$ does not come into play until $m_{H^{\pm}} \approx 100\ GeV$ for low values of $\tan\beta$ and $m_{H^{\pm}} \approx 150\ GeV$ for high values, $H^{\pm} \to c(b, s, d)$ dominates instead of $H^{\pm} \to \tau\nu$ for $m_{H^{\pm}} < m_t + m_b$. Note that only the method for calculating $\Gamma^{t^{*}b}_{H^{\pm}}$ has been altered in this paper; the method for calculating $\Gamma^{cb}_{H^{\pm}}$ and $\Gamma^{cs}_{H^{\pm}}$ have remained unchanged. The method that was used for the latter two partial widths approximates the resulting particles to be massless compared to the $H^{\pm}$. As the title suggests, these calculations were done in a flipped 2HDM.

8 Conclusion

This paper has explained how the off-shell partial width $H^\pm \to t^*\overline{d}_i \to W^\pm b\overline{d}_i$ can be calculated numerically and how the method can be been improved with various additions compared to earlier implementations in the 2HDMC program: first-order QCD-corrections, terms for high values of $\tan\beta$ and the $m_t^2\Gamma_t^2$-term has been included in the propagator. Finally, the method has been generalised to be applicable in models with FCNCs at tree level.

This improvement in how one can calculate the width $H^\pm \to t^*\overline{d}_i \to W^\pm b\overline{d}_i$ allows for more precise calculations, which in turn allows for more reliable constraints on the parameter space for 2HDMs. If more severe constraints can be set on 2HDMs it would allow the theory to be more easily confirmed or discarded as an incorrect description of our world.

We have also presented some examples of implications of these new calculations which show that in a type II model the $H^\pm \to t^*\overline{d}_i \to W^\pm b\overline{d}_i$-decay only contribute by a significant amount when $\tan\beta$ is small, a region in the parameter space that to a large extent is excluded. Although the contribution to the total width from $H^\pm \to t^*\overline{d}_i \to W^\pm b\overline{d}_i$ was not as great as initially and intuitively expected for these choices of parameters, there may still be some choices of values of parameters where it is significant enough so that one needs to take it into account. The effect on $BR(H^\pm \to \tau\nu)$ from these improvements have also been looked at, and the effect was found to be small. In a flipped model, on the other hand, the effects were large, especially for $\tan\beta = 50$.

8.1 Comparison of Old and New method

Even though the new method has several improvements over the fast one, it is still a good idea to use the fast method in certain intervals as the new method, while good, has very time-consuming calculations. The fast method stays true to its name and to calculate the partial width for a set of parameters is done in the blink of an eye, but the new method takes a few seconds. This may not seem like much if one only wants to calculate the width for only a few sets of parameters or has access to much computing power, but since the parameter space is so large one might need to do many calculations which can take hours, maybe even days. Far away from $m_{H^\pm} = m_t + m_b$, the difference between the two functions above the $m_{H^\pm} = m_t + m_b$ threshold is minuscule so one could use either, and when $m_{H^\pm} > m_t + m_b$ both functions are interpolated with the function that calculates the width in the approximation that all quarks are massless, i.e. $m_{H^\pm} \gg m_t + m_b$, so for very large $m_{H^\pm}$ there is not much difference between the two methods. It is only when one needs to work near $m_{H^\pm} = m_t + m_b$ it is really necessary to use the new one, if $m_{H^\pm} < m_t + m_b$ or $m_{H^\pm} > m_t + m_b$ is the region of study the fast method will do fine.

8.2 Outlook

Since this paper is mostly about the theory behind the calculation and the calculation itself there is much room left to compare results from the program with data from experiments. One might for example study the type II and flipped models in more detail and look at masses and $\sin(\beta-\alpha)$. As the program can now handle FCNCs one could study the effects and constraints from baryon decays such as $B \to D\tau\nu$.

Another improvement available for later projects is to include more QCD-corrections, or possibly improve and optimise the ones implemented by this project since they take a very long time to calculate. As the current corrections approximate the top quark to have a long lifetime they may not be very accurate for low $m_{H^\pm}$, so to calculate the corrections for the decay $H^\pm \to t^*b \to W^\pm bb$ would further improve the method for low $m_{H^\pm}$. If they were to take less time to calculate it would allow for more calculations to be done within a more reasonable timespan and thus one could investigate a larger region in the parameter space.

References

[1] G. Aad *et al.* [ATLAS Collaboration], Phys. Lett. B **716** (2012) 1 [arXiv:1207.7214 [hep-ex]].

[2] S. Chatrchyan *et al.* [CMS Collaboration], Phys. Lett. B **716** (2012) 30 [arXiv:1207.7235 [hep-ex]].

[3] G. Aad *et al.* [ATLAS Collaboration], JHEP **1503** (2015) 088 [arXiv:1412.6663 [hep-ex]].

[4] Gordon Kane, *Modern Elementary Particle Physics*, Perseus Publishing, Massachusetts, updated edition, 1993.

[5] T. D. Lee, Phys. Rev. D **8** (1973) 1226.

[6] David Griffiths, *Introduction to Elementary Particles*, Wiley-Vch, Weinheim, 2nd edition, 2008

[7] John Gunion *et. el The Higgs Hunter's Guide*, Westview Press, 2000

[8] commons.wikimedia.org/wiki/File : Mexican_hat_potential_polar_with_details.svg, Uploaded 2 Sep 2012

[9] O. Stål, Doctoral thesis, ISBN 978-91-554-7682-3, Uppsala University, 2009

[10] S. L. Glashow and S. Weinberg, Phys. Rev. D **15** (1977) 1958.

[11] D. Eriksson, J. Rathsman and O. Stal, Comput. Phys. Commun. **181** (2010) 189 [arXiv:0902.0851 [hep-ph]].

[12] J. Oredsson, *Properties of two Higgs Doublet Models in relation to data on $B \to D\tau\nu$*, Bachelor thesis, 2014

[13] A. Celis, V. Ilisie and A. Pich, JHEP **1312** (2013) 095 [arXiv:1310.7941 [hep-ph]].

[14] J. Abdallah *et al.* [DELPHI Collaboration], Eur. Phys. J. C **34** (2004) 399 [hep-ex/0404012].

[15] G. C. Branco, P. M. Ferreira, L. Lavoura, M. N. Rebelo, M. Sher and J. P. Silva, Phys. Rept. **516** (2012) 1 [arXiv:1106.0034 [hep-ph]].

[16] A. Djouadi and P. Gambino, Phys. Rev. D **51** (1995) 218 [Phys. Rev. D **53** (1996) 4111] [hep-ph/9406431].

Abbreviations

SM - Standard Model
2HDM - Two Higgs Doublet Model
2HDMC - Two Higgs Doublet Model Calculator
VEV - Vacuum Expectation Value
QCD - Quantum Chromodynamics
FCNC - Flavour Changing Neutral Current